

Optical sensing of square lattice photonic crystal point-shifted nanocavity for protein adsorption detection

Tsan-Wen Lu, Pin-Tso Lin, Kuan-Un Sio, and Po-Tsung Lee

Citation: *Applied Physics Letters* **96**, 213702 (2010); doi: 10.1063/1.3436550

View online: <http://dx.doi.org/10.1063/1.3436550>

View Table of Contents: <http://scitation.aip.org/content/aip/journal/apl/96/21?ver=pdfcov>

Published by the [AIP Publishing](#)

Articles you may be interested in

[Application of GaInNAs for the gain medium of a photonic crystal microcavity](#)

J. Vac. Sci. Technol. B **30**, 02B127 (2012); 10.1116/1.3691651

[Photonic crystal microdisk lasers](#)

Appl. Phys. Lett. **98**, 131109 (2011); 10.1063/1.3567944

[Photonic crystal slot nanobeam slow light waveguides for refractive index sensing](#)

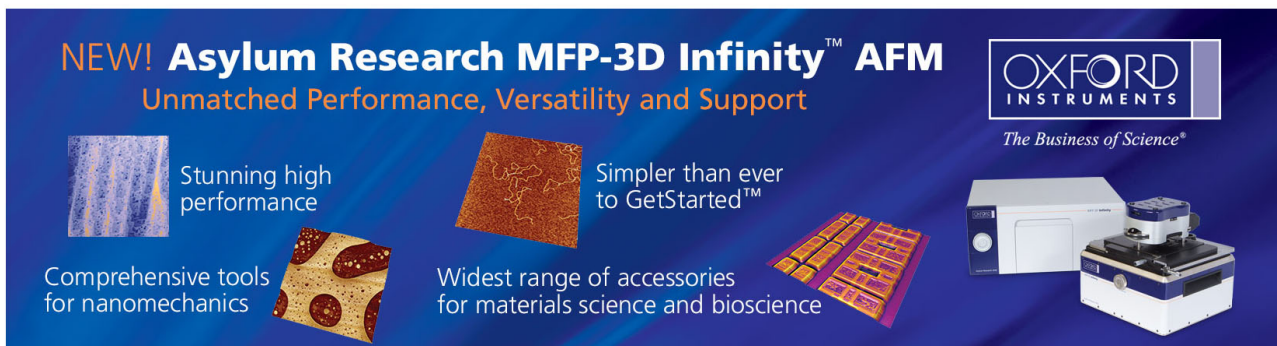
Appl. Phys. Lett. **97**, 151105 (2010); 10.1063/1.3497296

[Hybrid polymer-porous silicon photonic crystals for optical sensing](#)

J. Appl. Phys. **106**, 023109 (2009); 10.1063/1.3177344

[Laser characteristics with ultimate-small modal volume in photonic crystal slab point-shift nanolasers](#)

Appl. Phys. Lett. **88**, 211101 (2006); 10.1063/1.2206087



NEW! Asylum Research MFP-3D Infinity™ AFM
Unmatched Performance, Versatility and Support

OXFORD INSTRUMENTS
The Business of Science®

Stunning high performance

Simpler than ever to GetStarted™

Comprehensive tools for nanomechanics

Widest range of accessories for materials science and bioscience

Optical sensing of square lattice photonic crystal point-shifted nanocavity for protein adsorption detection

Tsan-Wen Lu,^{a)} Pin-Tso Lin, Kuan-Un Sio, and Po-Tsung Lee

Department of Photonics, Institute of Electro-Optical Engineering, National Chiao Tung University,
Rm. 415, CPT Building, 1001 Ta-Hsueh Road, Hsinchu 300, Taiwan

(Received 7 April 2010; accepted 4 May 2010; published online 24 May 2010)

We propose a point-shifted D_0 nanocavity formed by locally modulating four central air holes in square lattice photonic crystal for optical sensing application. Three defect modes in this nanocavity, including monopole, whispering-gallery, and dipole modes, are identified in experiments. We also apply a chemical treatment on InGaAsP surface to form a 1-octadecanethiol linking monolayer, which enables the following protein adsorption. In experiments, the wavelength shifts of lasing modes in the D_0 nanocavity due to the protein adsorption are observed and agree with the simulation results. This can be a practical tool for label-free molecule detection in biomedical researches.

© 2010 American Institute of Physics. [doi:10.1063/1.3436550]

Photonic crystal (PhC) nanocavity,^{1,2} hosts the advantage of well controlling photon flow in wavelength scale due to photonic band gap effect. In recent years, PhC nanocavities have been demonstrated with different functionalities, such as lasers,^{1,2} optical filters,³ nanoparticle manipulation,⁴ optical sensors,⁵⁻⁹ and so on. In these applications, optical sensing via optical resonances is quite attractive and interesting, which has long been a practical tool in chemical analysis, biomedics, environmental monitoring, and so on. Although optical sensing has been exhaustively developed by various photonic structures¹⁰ with relatively large sensing scale size ($>100 \mu\text{m}$) over past decades, optical sensors based on PhC nanocavities are expected to have advantages of high sensitivity, very compact sensing region size, very low analyte consumption (typically, $<1 \text{ fL}$), and so on. Due to the ultrasmall nanocavity size, that is, the wavelength-scale interaction region with the analyte, PhC nanocavities are potential in realizing condensed on-chip and microarray sensors. In recent years, various PhC nanocavities have been applied in index,⁵⁻⁷ nanoparticle,⁸ and protein⁹ sensing. Among these applications, the demonstration of protein sensing indicates the possibility of label-free molecule detection in biomedical researches. For detecting protein and virus with sizes from tens to hundreds of nanometers in diameter (for example, RNA-protein complex, Influenza virus A, etc.), the comparable size of PhC nanocavity (typically, several hundred nanometers) could lead the sensitivity down to single molecule, as achieved by other photonic structures recently.^{11,12}

Up to date, the protein sensing by PhC devices^{9,13} is mainly in passive way. Very little attention has been given to the usage of light emitting devices, for example, PhC light emitting diodes and lasers. In our recent work,¹⁴ we have proposed a square-PhC point-shifted D_0 nanocavity laser with lowest-order whispering-gallery (WG) mode. In this report, we experimentally identify the three defect modes in this nanocavity, which has not been investigated in our previous work yet. Then we make a chemical treatment on the nanocavity surface to enable the protein adsorption. In ex-

periments, we observe the wavelength shifts of lasing modes in D_0 nanocavity due to the protein adsorption, which are confirmed by the simulation results.

Scheme of square-PhC D_0 nanocavity design is shown in Fig. 1(a). The square PhCs are defined by air holes on a suspended dielectric slab. The positions and radii of four central air holes are shifted outward and shrunk to be r' , respectively, to form the nanocavity region. This design is realized on InGaAsP multiquantum-wells (MQWs) by electron-beam lithography and a series of reactive ion etching/inductively coupled plasma dry-etching process. The suspended slab structure is formed by HCl selective wet-etching process. Top- and tilted-view scanning electron microscope (SEM) pictures of the fabricated square-PhC D_0 nanocavity are shown in Figs. 1(b) and 1(c).

By three-dimensional (3D) finite-difference time-domain (FDTD) simulations, we find three defect modes in the D_0 nanocavity under different r' over lattice constant (a) (r'/a) ratios, including monopole, WG, and dipole modes. Figures 2(a) and 2(b) show the simulated relationship of mode frequency versus r'/a ratio and mode profiles in electrical fields of these three modes, respectively. To observe and identify these modes in experiments, we fabricate a square-PhC D_0 nanocavity array with increased r'/a ratio from 0.285 to 0.34, fixed r/a ratio of 0.37, and a of 530 nm. The nanocavities are optically pumped at room temperature with wavelength, pump spot diameter, pulse duty cycle, and pulse

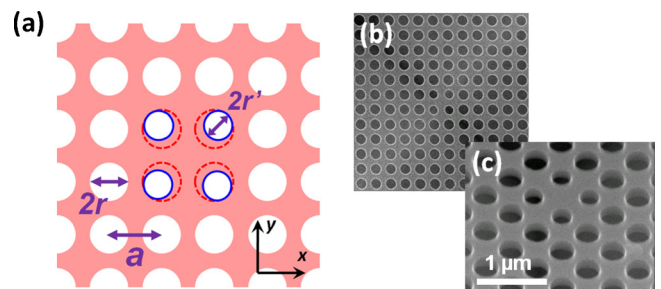


FIG. 1. (Color online) (a) Scheme of square-PhC D_0 nanocavity design. (b) Top- and (c) tilted-view SEM pictures of fabricated square-PhC D_0 nanocavity. The slab thickness, lattice constant, and r/a ratio are 180 nm, 530 nm, and 0.37, respectively.

^{a)} Author to whom correspondence should be addressed. Electronic mail: ricky.eo94g@nctu.edu.tw.

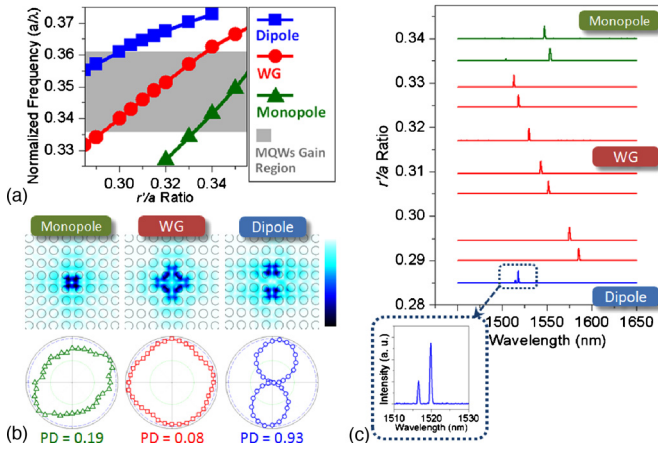


FIG. 2. (Color online) The simulated (a) relationship of mode frequency vs r'/a ratio and (b) mode profiles in electrical fields of monopole, WG, and dipole modes. The measured polarizations of monopole, WG, and dipole modes are shown in the bottom insets of (b). (c) The relationship between the measured single-mode lasing wavelength and r'/a ratio of square-PhC D_0 nanocavity. The bottom inset shows the splitting spectrum of the dipole mode.

width of 845 nm, $3.5 \mu\text{m}$, 0.2%, and 40 ns, respectively. The measured single-mode lasing wavelengths with different r'/a ratios of the D_0 nanocavity are shown in Fig. 2(c). Compared with the simulation results in Fig. 2(a), when r'/a ratio decreases, we can identify the lasing modes from top to bottom in Fig. 2(c) as monopole, WG, and dipole modes. To further confirm this identification, we measure their polarizations, as shown in the bottom insets of Fig. 2(b). For the identified dipole mode, we obtain a very high polarized degree (PD) of 0.93. We also observe the wavelength splitting as shown in the bottom inset of Fig. 2(c) due to degeneracy breaking of dipole mode caused by the fabrication imperfection. On the other hand, WG and monopole modes both show low PD values of 0.08 and 0.19, respectively, because of the far-field cancellations of x - and y -electrical fields. Thus, we can confirm the mode identification.

Optically sensing protein (antigen/antibody), DNA, and virus via optical resonators hosts the advantages of label-free, real-time monitoring, and so on. It simplifies the traditional process with fluorescence label and is beneficial for fundamental studies in biological process, drug discovery, disease diagnosis, and therapy. To apply our proposed device for protein sensing, first, we have to make a chemical treatment on InGaAsP surface to provide a linking layer at the organic/inorganic interface. Although various surface treatments on silica resonators have been reported, only little attention has been given to III-V semiconductor materials, whose main purpose is combining optical sensors and light emitting devices. In our experiments, we use 1-octadecanethiol [ODT, $\text{HS}(\text{CH}_2)_{17}\text{CH}_3$] as the linking layer. Due to the straight alkane chains shown in Fig. 3(a), ODT can form a very ordered monolayer on InP (Ref. 15) and GaAs (Ref. 16) surfaces by sulfur covalent attachments on indium and asinine. To form the ODT monolayer on InGaAsP surface, the process is illustrated below:

- (1) The InGaAsP surface is cleaned by acetone and isopropanol (IPA). It is then immersed in 48% hydrofluoric acid solution for 10 min to remove the native

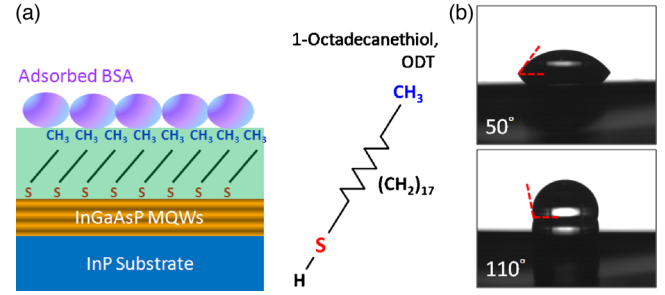


FIG. 3. (Color online) (a) Scheme of protein adsorption on ODT-treated InGaAsP surface. The chemical formula of ODT is also shown. (b) Measured contact angles of oxide-free InGaAsP surfaces before and after ODT treatment, which are 50° and 110° , respectively.

oxide on surface and permit the following ODT monolayer formation.

- (2) After rinsed by deionized water and IPA, the surface is incubated in 0.15 mM ODT/ethanol solution for 40 h. Then the surface is rinsed and dried by ethanol to remove unattached ODT residue.
- (3) The surface with ODT monolayer is then incubating in bovine serum albumin (BSA)/phosphate buffered saline with 1 mg/mL concentration for 1 h. Finally, the sample is rinsed by deionized water to remove weakly adsorbed BSA residue and dried.

The surface becomes hydrophilic again, which indicates the protein adsorption. The overall scheme is shown in Fig. 3(a).

The square-PhC D_0 nanocavities with different r'/a ratios on the same wafer measured in Fig. 2(c) are treated by above process. The ODT-treated D_0 nanocavities are optically pumped by fixed power of 0.6 mW at room temperature and single-mode lasing wavelengths of each defect mode are recorded before and after BSA adsorption. The measured spectra are shown in Fig. 4(a). The monopole, WG, and dipole modes show redshifts of 2.0 nm, 1.8 nm, and 1.2 nm in wavelength, respectively, which are arisen from the adsorbed protein on the D_0 nanocavity. To further confirm these observations, we apply 3D FDTD method to simulate the wavelength shifts of each mode. We assume^{9,13} that the protein adsorbs on the entire surface of the D_0 nanocavity, including air hole sidewall, top, and bottom surfaces, as illustrated in Fig. 4(b), where the adsorbed protein is assumed to be with refractive index of 1.5 and uniform effective thickness varied from 0 to 2 nm. The simulated wavelength shifts of monopole, WG, and dipole modes are shown in Fig. 4(c). By matching the measured results with the simulated ones, we can obtain an effective protein thickness of 1.55 nm,^{9,17} where the wavelength shifts of monopole, WG, and dipole modes are 2.0 nm, 1.8 nm, and 1.7 nm, respectively. Besides, considering the ultrasmall nanocavity size in several hundreds of nanometers and defect mode field distribution of only four-lattice-period distance from the D_0 nanocavity, the

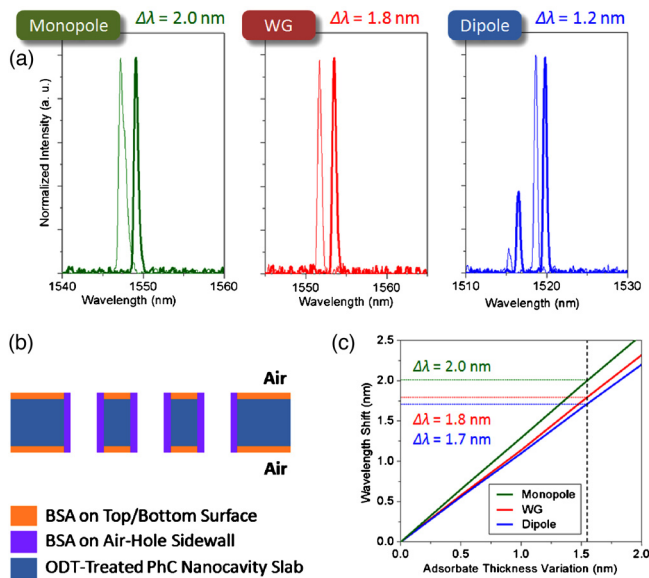


FIG. 4. (Color online) (a) The measured single-mode lasing spectra of monopole, WG, and dipole modes (from left to right) before (solid-line) and after (bold solid-line) the protein (BSA) adsorption. (b) Scheme of protein adsorption on the entire surface of square-PhC D_0 nanocavity, including air hole sidewall, top, and bottom surfaces. (c) 3D FDTD simulated wavelength shifts of monopole, WG, and dipole modes (from top to bottom) contributed from the adsorbed protein on the entire D_0 nanocavity surface. The r'/a ratios of D_0 nanocavities in simulations are set to be 0.34, 0.30, and 0.28 for monopole, WG, and dipole modes.

interrogated analyte amount estimated can be less than 2.2 fg. Furthermore, when we consider the spectral line width of the lasing mode in experiments, for example, 0.6 nm for WG mode, the minimum measurable protein amount can be less than 0.8 fg (~ 7300 BSA molecules), which indicates the high sensitivity of our device. Since the detection of protein adsorption is demonstrated, we believe sensing of functionalized protein binding can be achieved in the near future. This initial demonstration strongly indicates that the PhC nanocavity lasers can serve as highly sensitive and label-free optical sensors in fundamental studies of biological researches.

In summary, we propose a point-shifted D_0 nanocavity formed by shifting and shrinking the four central air holes of square-PhC for protein adsorption detection. Three simulated defect modes in the D_0 nanocavity under different r'/a ratios, including monopole, WG, and dipole modes, are identified by lasing wavelengths and polarizations in experiments. We also apply a chemical treatment on InGaAsP

surface to form the ODT linking monolayer, which enables the following protein (BSA) adsorption. In experiments, the wavelength shifts of lasing modes due to the BSA adsorption are observed. Compared with the FDTD simulation results, we can estimate the effective thickness of adsorbed protein to be 1.55 nm. Very small measurable protein amount less than 0.8 fg can be achieved through WG mode in this nanocavity. These observations strongly indicate this light emitting nanocavity laser is capable of sensing advanced functionalized protein binding and can serve as a highly sensitive, label-free, and ultracompact optical sensor in fundamental studies of biological process, drug discovery, disease diagnosis, and therapy.

This work is supported by Taiwan's National Science Council (NSC) under Contract Nos. NSC-98-2120-M-009-002 and NSC-98-2221-E-009-015-MY2. The authors would like to thank the help from Center for Nano Science and Technology (CNST) of National Chiao Tung University (NCTU), Taiwan. The author Tsan-Wen Lu would like to give his special thanks to Miss Mong-Ting Lien and Professor Jui-Chou Hsu in Institute of Molecular Medicine, National Tsing Hua University (NTHU), Taiwan, for their generous help and fruitful discussions.

- ¹O. Painter, R. K. Lee, A. Scherer, A. Yariv, J. D. O'Brien, P. D. Dapkus, and I. Kim, *Science* **284**, 1819 (1999).
- ²K. Nozaki, S. Kita, and T. Baba, *Opt. Express* **15**, 7506 (2007).
- ³B.-S. Song, T. Asano, Y. Akahane, Y. Tanaka, and S. Noda, *J. Lightwave Technol.* **23**, 1449 (2005).
- ⁴M. Barth and O. Benson, *Appl. Phys. Lett.* **89**, 253114 (2006).
- ⁵S. Kita, K. Nozaki, and T. Baba, *Opt. Express* **16**, 8174 (2008).
- ⁶T. Sünner, T. Stichel, S. H. Kwon, T. W. Schlereth, S. Höfling, M. Kamp, and A. Forchel, *Appl. Phys. Lett.* **92**, 261112 (2008).
- ⁷A. Di Falco, L. O'Faolain, and T. F. Krauss, *Appl. Phys. Lett.* **94**, 063503 (2009).
- ⁸M. R. Lee and P. M. Fauchet, *Opt. Lett.* **32**, 3284 (2007).
- ⁹M. R. Lee and P. M. Fauchet, *Opt. Express* **15**, 4530 (2007).
- ¹⁰X. Fan, I. M. White, S. I. Shopova, H. Zhu, J. D. Suter, and Y. Sun, *Anal. Chim. Acta* **620**, 8 (2008).
- ¹¹A. M. Armani, R. P. Kulkarni, S. E. Fraser, R. C. Flagan, and K. J. Vahala, *Science* **317**, 783 (2007).
- ¹²F. Vollmer, S. Arnold, and D. Keng, *Proc. Natl. Acad. Sci. U.S.A.* **105**, 20701 (2008).
- ¹³S. C. Buswell, V. A. Wright, J. M. Buriak, V. Van, and S. Evoy, *Opt. Express* **16**, 15949 (2008).
- ¹⁴T. W. Lu, P. T. Lin, K. U. Sio, and P. T. Lee, *Opt. Express* **18**, 2566 (2010).
- ¹⁵H. H. Park and A. Ivanisevic, *J. Phys. Chem. C* **111**, 3710 (2007).
- ¹⁶C. L. McGuinness, A. Shaporenko, C. K. Mars, S. Uppili, M. Zharnikov, and D. L. Allara, *J. Am. Chem. Soc.* **128**, 5231 (2006).
- ¹⁷H. P. Wampler and A. Ivanisevic, *Micron* **40**, 444 (2009).